Transcriptomic analysis and physiological characteristics of exogenous naphthylacetic acid application to regulate the healing process of oriental melon grafted onto squash

Chuanqiang Xu [Corresp., 1, 2, 3], **Fang Wu** [1, 2, 3], **Jieying Guo** [1, 2, 3], **Shuan Hou** [1, 2, 3], **Xiaofang Wu** [1, 2, 3], **Ying Xin** [1, 2, 3]

[1] National & Local Joint Engineering Research Center of Northern Horticultural Facilities Design & Application Technology (Liaoning), Shenyang, China

[2] Key Laboratory of Protected Horticulture (Shenyang Agricultural University) Ministry of Education, Shenyang, China

[3] College of Horticulture, Shenyang Agricultural University, Shenyang, China

Corresponding Author: Chuanqiang Xu
Email address: chuanqiang79@syau.edu.cn

The plant graft healing process is an intricate development influenced by numerous endogenous and environmental factors. This process involves the histological changes, physiological and biochemical reactions, signal transduction, and hormone exchanges in the grafting junction. Studies have shown that applying exogenous plant growth regulators can effectively promote the graft healing process and improve the quality of grafted plantlets. However, the physiological and molecular mechanism of graft healing formation remains unclear. In our present study, transcriptome changes in the melon and cucurbita genomes were analyzed between control and NAA treatment, and we provided the first view of complex networks to regulate graft healing under exogenous NAA application. The results showed that the exogenous NAA application could accelerate the graft healing process of oriental melon scion grafted onto squash rootstock through histological observation, increase the SOD, POD, PAL, and PPO activities during graft union development and enhance the contents of IAA, GA_3, and ZR except for the IL stage. The DEGs were identified in the plant hormone signal-transduction, phenylpropanoid biosynthesis, and phenylalanine metabolism through transcriptome analysis of CK *vs.* NAA at the IL, CA, and VB stage by KEGG pathway enrichment analysis. Moreover, the exogenous NAA application significantly promoted the expression of genes involved in the hormone signal-transduction pathway, ROS scavenging system, and vascular bundle formation.

Transcriptomic analysis and physiological characteristics of exogenous naphthylacetic acid application to regulate the healing process of oriental melon grafted onto squash

Chuanqiang Xu[1,2,3*], Fang Wu[1,2,3], Jieying Guo[1,2,3], Shuan Hou[1,2,3], Xiaofang Wu[1,2,3] , Ying Xin[1,2,3]

[1] College of Horticulture, Shenyang Agricultural University, Shenyang 110866, China

[2] National & Local Joint Engineering Research Center of Northern Horticultural Facilities Design & Application Technology (Liaoning), Shenyang 110866, China

[3] Key Laboratory of Protected Horticulture (Shenyang Agricultural University) Ministry of Education, Shenyang 110866, China

* Correspondence:

chuanqiang79@syau.edu.cn (CX)

Abstract

The plant graft healing process is an intricate development influenced by numerous endogenous and environmental factors. This process involves the histological changes, physiological and biochemical reactions, signal transduction, and hormone exchanges in the grafting junction. Studies have shown that applying exogenous plant growth regulators can effectively promote the graft healing process and improve the quality of grafted plantlets. However, the physiological and molecular mechanism of graft healing formation remains unclear. In our present study, transcriptome changes in the melon and cucurbita genomes were analyzed between control and NAA treatment, and we provided the first view of complex networks to regulate graft healing under exogenous NAA application. The results showed that the exogenous NAA application could accelerate the graft healing process of oriental melon scion grafted onto squash rootstock through histological observation, increase the SOD, POD, PAL, and PPO activities during graft union development and enhance the contents of IAA, GA_3, and ZR except for the IL stage. The DEGs were identified in the plant hormone signal-transduction, phenylpropanoid biosynthesis, and phenylalanine metabolism through transcriptome analysis of CK *vs.* NAA at the IL, CA, and VB stage by KEGG pathway enrichment analysis. Moreover, the exogenous NAA application significantly promoted the expression of genes involved in the hormone signal-transduction pathway, ROS scavenging system, and vascular bundle formation.

Keywords: oriental melon, squash, graft, exogenous naphthylacetic acid, transcriptomic analysis, endogenous hormone, signal transduction, ROS scavenging, vascular bundle formation.

Introduction

Grafting is a widely used technology to help horticultural plants overcome their limiting growth and reproduction factors (Lee et al., 2010). In cultivation, the most frequently consumed horticulture plants, such as melon, watermelon, tomato, eggplant, and cucumber, are often grafted (Pina & Errea, 2005; Zheng et al., 2010). Successful grafting is a complex process involving the

initial adhesion of scion and rootstock, callus tissue formation, and vascular bundle connection during the graft healing process. Callus tissue formation at the graft interface initiates the grafting process, and a lack of callus tissue formation can lead to grafting failure (Pina & Errea, 2005). In addition, the callus cells differentiating into vascular tissue to re-connect the xylem and phloem at the graft junction is an essential process for successful grafting (Flaishman et al., 2008). A functional vascular connection is an important signal for the establishment of successful graft healing (Turquois & Malone, 1996; Fernández-garcía et al., 2004). However, the reconnection of the rootstock and the scion has tissue asymmetry. The phloem junction occurs at the graft junction before the xylem (Melnyk et al., 2015).

As we all know, complex physiological metabolites occur during the graft healing process (Koepke & Dhingra, 2013). Even though the studies on the histological analysis and physiological and biochemical changes of graft healing have been reported (Chen et al., 2017; Cookson et al., 2013), the comprehensive understanding of the molecular mechanism of successful graft healing remains insufficient. The genome-wide transcriptome analysis could help to clarify the specific and underlying molecular mechanisms of grafting-depended biochemical processes. Some studies showed that transcriptomics efficiently analyzed the graft healing process of the different species. In the graft healing process of grapevine, transcriptional changes were examined via whole-genome microarray analysis, and the report revealed many genes associated with cell wall modification, hormone signaling, secondary metabolism, and wound responses (Cookson et al., 2013). Transcriptomic analysis of graft healing in Litchi showed nine annotated unigenes that participated in the auxin signaling pathway had higher expression levels in the compatible grafts than incompatible ones (Chen et al., 2017). In the graft healing process of hickory, the transcriptomic analysis revealed 112 candidate uniqueities, which participated in the auxin and cytokinin signaling pathways (Qiu et al., 2016). Genome-wide transcriptome analysis of tissues above and below graft junctions revealed that the inter-tissue communication process occurred independently of functional vascular connections and acted as a signal to activate vascular regeneration (Melnyk et al., 2018).

Phytohormones play an essential role in plant wound healing and vascular formation (Melnyk et al., 2015)[7]. Through the exogenous auxin application to callus, the formation of xylem and phloem was enhanced effectively (Wetmore & Rier, 1963; Scarpella et al., 2006). The application of exogenous phytohormones, such as heteroauxin and zeatin, positively accelerated the healing by increasing the vascular bundle formation rate (Lu & Song, 1999). In the grafted seedlings cultivation practice, studies showed that applying exogenous plant growth regulators could effectively promote the healing of grafted seedlings, shorten the healing period of grafting, and improve the quality of grafted seedlings. Some plant growth regulators, like an auxin-based plant growth regulator, naphthylacetic acid (NAA), commonly treat scions or rootstocks to accelerate graft healing. However, the physiological and molecular mechanism of graft healing by exogenous NAA application is not comprehensive. The main goals of the present study aimed to characterize the anatomical development stages of graft healing formation and clarify the physiological and transcriptomic changes in the graft junction of oriental melon grafted onto squash under NAA

application, and provide a theoretical and practical basis for further improving the efficiency of commercial grafted melon seedlings cultivation.

Materials and methods

Experimental materials

In the present study, we took the oriental melon cultivar (YinQuan No.1, *Cucumis melo var. Makuwa* Makino) to graft onto the squash cultivar (ShengZhen No.1, *C. moschata*) by splicing graft method when the scion's first-true-leaf fully expanded and rootstock's cotyledon development stage, using the one-cotyledon method (Davis et al., 2008). During the grafting process, the grafted seedlings of scions dipped in the NAA solution (40 $mg \cdot L^{-1}$) were the treatments (NAA), and dipping in the distilled water were the controls (CK). Grafted seedlings were transplanted in the nutritional bowl (12 cm×12 cm) and moved into the healing chamber for grafted seedlings cultivation at Shenyang Agriculture University. The management methods of grafted seedlings for CK and NAA were consistent (Liu et al., 2017).

Paraffin sectioning and microscopy

The samples of 0.3-0.5cm stem above and below the graft junction were fixed, softened, dehydrated, infiltrated, and embedded in paraffin during graft union development (Ribeiro et al., 2015). Transverse serial sections (≈10μm thickness) were stained with pH4.4 toluidine blue (O'Brien et al., 1964), and mounted using synthetic resin (Permount). Sections were examined using a light microscope (Lecia RM 2245, Germany). After observing the paraffin section, the IL, CA, and VB stage of CK and NAA was respectively screened, and the corresponding samples carried out the other experiments for measuring the activities of enzymes involved in ROS scavenging (SOD, POD, PAL, and PPO), endogenous hormones contents (IAA, GA_3, and CTK), and RNA-seq assay.

Determination of SOD, POD, PAL, and PPO activities

The graft junction tissues (≈0.5 g) of CK and NAA at the IL, CA, and VB stage with three biological replicates were ground with a pestle in an ice-cold mortar with 4 ml 50 mM phosphate buffer (pH 7.0). The homogenates were centrifuged at 12,000 rpm for 20 min at 4°C, and the supernatant was used to measure enzyme activities (Mishra et al., 2006). SOD activity was assayed by measuring its ability to inhibit the photochemical reduction of nitro blue tetrazolium. POD activity was measured as the increase in absorbance at 470 nm caused by guaiacol oxidation (Polle et al., 1994). PAL activity was measured (Sánchez-Rodríguez et al., 2011). The reaction mixture was 0.4 ml of 100 mM Tris-HCl buffer (pH 8.8), 0.2 ml of 40 mM phenylalanine, and 0.2 ml of enzyme extract. The reaction mixture was incubated for 30 min at 37℃ and the reaction was ended by adding 25% trichloroacetic acid. The absorbance of the supernatant was measured at 280 nm. PPO activity was spectrophotometrically determined at 398 nm (Olmos et al., 1997). The reaction mixture contained 2.8 ml 0.1% catechol solution, and 0.2 ml enzyme extract in a total volume of 3 ml.

Determination of hormones content by ELISA

We sampled the graft junction tissues of CK and NAA at the IL stage, CA stage, and VB stage with three biological replicates. The content of IAA, GA_3, and ZR was measured by the Enzyme-

Linked Immunosorbent Assay (ELISA), and the detailed protocol for determining the hormone content was previously described (Yang et al., 2001). GC-MS and HPLC validated the accuracy of ELISA kits (China Agricultural University).

RNA Extraction, Library Construction, and Sequencing

Total RNA extraction, library construction, and RNA-Seq were performed by Biomarker Technology Co. (Beijing, China, https://www.biocloud.net/). RNA concentration was measured using NanoDrop 2000 (Thermo), and the detailed protocol was previously described (Xu et al., 2021). The raw sequencing data had been uploaded to the NCBI Sequence Read Archive (SRA) with the accession number PRJNA655799 and PRJNA689873.

Differential Expression Analysis

We respectively performed Melon (DHL92) v3.6.1 Genome and Cucurbita moschata (Rifu) Genome (http://cucurbitgenomics.org) to analyze the raw sequencing data of graft junction of CK and NAA at IL, CA, and VB stage. Differential expression analysis of two conditions/groups was performed using the DEseq. DEseq provides statistical routines for determining differential expression in digital gene expression data using a model based on the negative binomial distribution. The resulting *p*-values were adjusted using Benjamini and Hochberg's approach for controlling the false discovery rate. Genes with an adjusted p-value <0.01 found by DEseq were assigned as differentially expressed (Zhang et al., 2018).

Enrichment Analysis of GO Enrichment and KEGG Pathway

Gene Ontology (GO) enrichment analysis of the differentially expressed genes (DEGs) was implemented by the GO seq R packages based on Wallenius non-central hyper-geometric distribution (Young et al., 2010), which can adjust for gene length bias in DEGs. KEGG is a database resource for understanding high-level functions and utilities of the biological system, such as the cell, the organism, and the ecosystem, from molecular-level information, especially large-scale molecular datasets generated by genome sequencing and other high-throughput experimental technologies (http://www.genome.jp/kegg/). We used KOBAS software to test the statistical enrichment of differential expression genes in KEGG pathways (Mao et al., 2005).

Quantitative real-time PCR (qRT-PCR)

Some differentially expressed genes were selected to validate the accuracy of RNA-Seq data using qRT-PCR preparation with three biological replicates for each sample was conducted as described above. According to the manufacturer's instructions, the first-strand cDNA synthesis kit was performed using a Prime-Script™ II First Strand cDNA synthesis kit (Takara Bio, Dalian, China). The primer sets for each unigenes were designed by Primer Premier 5.0. qRT-PCR was carried out on Yena Real-Time PCR System (qTOWER3/qTOWER3 touch, Germany) with SYBR Premix Ex Taq™ II kit (Takara).

Statistical Analysis

The data were displayed with the mean±standard error in triplicate and analyzed by a-way variance (ANOVA, SPSS 22.0 software). Significant analysis was performed by Duncan's multiple range tests ($p<0.05$). The figures were produced by PRISM 8.0 software.

Results

Effects of exogenous NAA application on histological changes of graft junction

A significant adhesion was observed in the graft junction of oriental melon grafted onto squash at 2 DAG (Figure 1A, 1D). The isolation layer (IL)was generally formed by the protoplasm of destructed parenchyma cells and dead cells on the wound interface (Yang et al., 2016). The results showed that exogenous NAA application could not promote the formation of an isolated layer. With the graft junction development, the isolation layer gradually disappeared. Callus tissue (CA) provides a pathway for the communication between scion and stock (Wang & Kollmann, 1996). The graft junction with exogenous NAA treatment formed a callus tissue at 5 DAG (Figure 1E), while the callus formation of CK was observed at 6 DAG (Figure 1B). The vascular connection between the grafted partners was a mark of grafting success (Pina et al., 2005; Olmstead et al., 2006). At 8 DAG (Figure1F), the graft junction with exogenous NAA treatment formed vascular bundles (VB), and the new vascular bundle formation of CK occurred at 9 DAG (Figure 1C). The results suggested that exogenous NAA application could shorten the graft healing process of oriental melon seedlings grafted onto squash.

Effects of exogenous NAA application on the activities of the related enzyme involved in ROS scavenging of graft junction during graft union development

In higher plants, mechanical wounding generates ROS production, and the antioxidant enzyme activities in the graft junction interface may be responsible for the degradation of the grafting zone (Aloni et al., 2008; Ireneusz et al., 2008; Irisarri et al., 2015; Xu et al., 2015). Along with the graft union development, SOD activities of CK and NAA treatment first rose and then fell and presented the highest activity at the CA stage. SOD activity of NAA treatment was significantly higher than CK at the IL and CA stage (Figure 2A). POD activity was significantly higher than CK at the CA stage and reached the highest activity under NAA treatment (Figure 2B). In CK, POD activity was the highest value, and no significant difference compared with NAA treatment at the VB stage. As shown in Figure 2C, NAA treatment increased PAL activity during the graft healing process. PAL activity was significantly higher than CK except for the CA stage and reached the highest activity at the VB stage. PPO activity had a similar change trend in CK and NAA, which increased. Under NAA treatment, the value was significantly higher than CK at the IL stage. There were no significant differences in PPO activity at the CA and VB stages between CK and NAA treatment.

Effects of exogenous NAA application on endogenous hormones contents of graft junction during graft union development

Some major endogenous hormones, IAA, CTK, and GA, relate to callus formation development and vascular bundle reconnection (Nieminen et al., 2008; Mauriat & Moritz, 2009; Bishopp et al., 2011). Our results indicated that exogenous NAA application accelerated the graft healing process by promoting the content of three endogenous hormones at three critical stages. During the early stage of graft healing, a block in auxin basipetal transport was generated due to vascular damage, and the content showed a decreased trend. As the healing process was completed, auxin was accumulated in the wound interface and the content gradually increased. Under NAA treatment, the auxin content was lower than CK at the IL stage and was significantly higher than CK at the CA and VB stages (Figure 3A). The GA_3 content was significantly increased in CK at the CA and

VB stage, while there was no significant difference at the IL stage. When exogenous NAA was applied, the changing trend of GA_3 content was consistent with CK and significantly higher than CK at the VB stage (Figure 3B), which was 1.25 times that of CK. The content of ZR gradually increased during the graft healing process and reached the highest value in CK at the VB stage. Under NAA treatment, the trend of ZR content was consistent with CK, and the ZR content was significantly higher than CK at the CA and VB stages, which was 1.3 and 1.2 times that of CK, respectively (Figure 3C).

Identification of differentially expressed genes (DEGs) of graft junction under exogenous NAA application during graft union development

In order to further study the molecular mechanism of exogenous NAA application to regulate the graft healing process of oriental melon grafted onto squash, we performed transcriptomic analysis of graft junction tissue at the IL, CA, and VB stage under exogenous NAA application. We identified the DEGs in the melon genome (Figure 4A) and Cucurbita moschata (Rifu) genome (Figure 4B), respectively, according to the criteria of at least two-fold change and FDR<0.01. The 5324 DEGs were discovered by analyzing CK *vs.* NAA in the melon genome (Figure 4A), with 1621 up-regulated and 1414 down-regulated at the IL stage; 261 up-regulated and 296 down-regulated at the CA stage; with 815 up-regulated and 917 down-regulated at the VB stage. 6602 DEGs were identified by analyzing CK *vs.* NAA in the cucurbita moschata (Rifu) genome (Figure 4B), with 696 up-regulated and 914 down-regulated at the IL stage; with 512 up-regulated and 1477 down-regulated at the CA; with 1574 up-regulated and 1429 down-regulated at the VB stage.

Gene ontology and pathway enrichment Analyses DEGs induced by exogenous NAA during graft union development

We used the Gene Classification System (GO) to further analyze the identified DEGs at the IL, CA, and VB stage under exogenous NAA treatment. The results showed that most DEGs were classified into three categories: biological process, cellular component, and molecular function (Figure 5). At the IL, CA, and VB stage (Figure 5A, 5C, 5E), there most highly enriched terms in the Melon genome were metabolic process (1270, 206, 693 genes), single-organism process (1142, 196, 609 genes) and cellular process (829, 153, 454 genes) within the biological process category; cell (804, 152, 509 genes), cell part (824, 124, 432 genes) and membrane part (801, 119, 424 genes) within the cellular component; binding (1031, 186, 586 genes), catalytic activity (1041, 200, 605 genes), and transporter activity (162, 42, 108 genes) within the molecular function category. Furthermore, at the IL, CA, and VB stage (Figure 6B, 6D, 6F), there most abundant terms in the Cucurbita moschata (Rifu) genome were metabolic process (540, 836, 1163 genes), single-organism process (453, 709, 847 genes) and cellular process (504, 768, 1129 genes) within the biological process category; cell (321, 538, 843 genes), cell part (321, 538, 843 genes) and organelle (222, 366, 638 genes) within the cellular component; binding (395, 561, 769 genes), catalytic activity (494, 725, 845 genes), and transporter activity (79, 80, 114 genes) within the molecular function category.

The DEGs were also subjected to KEGG pathway enrichment analysis. The top 20 pathways, which highest enrichment level based on the numbers and enrichment levels of the annotated

DEGs, were shown in Figure 6. The results were consistent with the results of GO functional analysis. It was noteworthy that plant hormone signal-transduction, phenylpropanoid biosynthesis, and phenylalanine metabolism were the overlapping pathways identified at the IL, CA, and VB stage under exogenous NAA treatment, respectively. At the IL stage (Figure 6A, 6B), 53 DEGs, 18 DEGs (using Melon genome), and 33 DEGs, 20 DEGs (using Cucurbita moschata genome) were involved in plant hormone signal transduction and phenylpropanoid biosynthesis, respectively. At the CA stage (Figure 7C) and VB stage (Figure 6E), we found that 12 DEGs, 10 DEGs, and 34 DEGs, 21 DEGs were enriched in plant hormone signal transduction and phenylpropanoid biosynthesis using Melon genome. However, 45 DEGs, 20 DEGs (Figure 6D), 38 DEGs, 20 DEGs (Figure 6F) were involved in phenylpropanoid biosynthesis and phenylalanine metabolism using Cucurbita moschata genome.

Exogenous NAA activated hormone signal-transduction pathway during graft union development

Plant hormones of scion-rootstock communication are critical for successful graft (Melnyk et al., 2015). In our study, IAA, GA_3, and ZR contents of graft junction increased under exogenous NAA application during graft union development (Figure 3), and most DEGs were enriched in the hormone signal-transduction pathway (Figure 6). So we analyzed the unigenes that participated in the hormone signal-transduction under exogenous NAA application (Figure 7). At the IL stage, four unigenes encoding auxin efflux carrier (MELO3C019102.2, CmoCh11G003520, CmoCh04G021920, CmoCh11G003180), three unigenes encoding auxin response factors (ARFs) (MELO3C003768.2, MELO3C025777.2, MELO3C019801.2), five unigenes encoding AUX/IAA (MELO3C007691.2, MELO3C024699.2, MELO3C004382.2, CmoCh10G006330, CmoCh09G004620), two unigenes encoding GH3 (MELO3C008672.2, MELO3C017825.2) were significantly up-regulated in auxin signaling. And three unigenes encoding type-B ARR protein (MELO3C012031.2, CmoCh15G008650, CmoCh05G000700), one unigene encoding CRE1 (CmoCh15G009250) and two unigenes encoding AHP (MELO3C024439.2, CmoCh14G013260) in cytokinin signaling were also greatly up-regulated. At the CA stage, one unigene encoding ARF (MELO3C033303.2) in auxin signaling, one unigene encoding type-B ARR protein (CmoCh14G016360) and four unigenes encoding AHP (CmoCh14G016980, CmoCh17G002800, CmoCh14G013260, CmoCh06G014530) were significantly up-regulated. At the VB stage, one unigene encoding auxin efflux carrier (CmoCh07G011410), one unigene encoding ARF (CmoCh08G001220), three unigenes encoding AUX/IAA (MELO3C025308.2, CmoCh07G006010, CmoCh14G018090), four unigenes encoding GH3 (MELO3C016616.2, MELO3C007597.2, CmoCh03G009710, CmoCh16G003520) in auxin signaling, and one unigene encoding type-B ARR protein (CmoCh15G008650), two unigenes encoding AHP (MELO3C024439.2, MELO3C015359.2) were significantly up-regulated, respectively. However, we found that exogenous NAA application did not significantly activated unigenes expression involved in GA signaling.

Exogenous NAA application activated expression of genes involved in Reactive Oxygen Species (ROS) Scavenging during graft union development

The efficient antioxidant defense system plays a vital role in the graft healing process and is necessary for successful grafting. Under exogenous NAA application, we found many DEGs involved in ROS scavenging, including unigenes encoding peroxidase (POD), ascorbate peroxidase (APX), peroxiredoxin (Prx), superoxide dismutase (SOD), and phenylalanine ammonia-lyase (PAL) were activated during graft union development (Figure 8). At the IL stage, eleven genes expression of POD, one gene expression of APX, two genes expression of Prx, one gene expression of SOD, and two genes expression of PAL were up-regulated by exogenous NAA application. At the CA stage, three genes expression of POD were up-regulated. Moreover, at the VB stage, five genes expression of POD, one gene expression of APX, two genes expression of Prx, two genes expression of SOD, and one gene expression of PAL were up-regulated.

Exogenous NAA application activated expression of genes related to vascular bundle formation during graft union development

It is well-known that the vascular bundle re-connection is a mark of successful grafting (Pina & Errea, 2005). In our study, exogenous NAA application accelerated the healing of oriental melon scion grafted onto the squash rootstock. In order to clarify the genes related to the vascular bundle formation process, including the cell elongation, vascular cell differentiation, and developing vascular cell trigger programmed cell death (PCD), we performed the heat map analysis of different unigenes expression (Figure 9), such as expansion, tubulin, cellulose synthase, cinnamoyl-CoA reductase (CCR), hydrolytic enzyme (aspartic proteinase, cysteine proteinase), nuclease (exonuclease, ribonuclease), metacaspases and MYB transcription factors, using transcriptome data (Figure 10). Enzymes such as expansions are necessary for cell growth and cell wall architecture (Ye & Zhong, 2015). The results showed that six unigenes encoding expansion (MELO3C017181.2, MELO3C025095.2, CmoCh11G001730, CmoCh01G005150, CmoCh03G004350, CmoCh10G002140) were up-regulated at the VB stage. Tubulin is involved in cell expansion by guiding nascent cellulose microfibrils deposition during vascular development (Mendu & Silflow, 1993; Mo et al., 2018). We found that the expression of five tubulin genes (CmoCh03G009120, CmoCh07G010840, CmoCh14G000910, CmoCh07G006190,CmoCh16G003240) were also elevated by exogenous NAA application at the VB stage, but CmoCh03G009120, CmoCh07G010840, CmoCh14G000910, and CmoCh07G006190, except CmoCh16G003240, were down-regulated at the CA stage. We identified four unigenes, encoding cellulose synthase (MELO3C016270.2, CmoCh16G005790, CmoCh09G010200, CmoCh14G009470) implicated in cellulose synthesis, were significantly up-regulated at the VB stage. One unigene encoding CCR (MELO3C017061.2) involved in the phenylpropanoid pathway was up-regulated at the IL and VB stages. Furthermore, five unigenes encoding aspartic proteinase (MELO3C020328.2, CmoCh15G014930, CmoCh07G004000, CmoCh04G013980, CmoCh18G008610), two unigenes encoding cysteine proteinase (MELO3C027001.2, CmoCh03G010910), one unigene encoding exonuclease (CmoCh13G010360), and tow unigenes encoding ribonuclease (MELO3C023673.2, CmoCh03G010620), all of them involved in xylogenesis (Iliev & Savidge, 1999; Courtois-Moreau et al., 2009; Iakimova & Woltering, 2017; Mo et al., 2018), were up-regulated at the VB stage.

Meanwhile, one unigene encoding metacaspases (CmoCh11G014810) that participated in PCD was also up-regulated at the VB stage. Additionally, sixteen unigenes encoding MYB transcription factors involved in the phenylpropanoid biosynthesis pathway were identified and significantly up-regulated by exogenous at the VB stage.

Validation of RNA-Seq data by qRT-PCR

To verify the DEGs related to hormone signal and phenylpropanoid biosynthesis identified using RNA-Seq, we performed qRT-PCR assays with independent samples collected from graft junction tissues at different graft healing stages. The expression levels of these selected ten genes were identified between the two data sets (Figure 10). The result showed that the expression of ten genes detected by qRT-PCR matched the trend of their FPKM value change in RNA-Seq.

Discussion

Some reports showed that exogenous auxin application could promote callus formation (Sacha, 1981; Enrico et al., 2006). We found that exogenous NAA application accelerated the callus formation time and effectively promoted the time of vascular bundles connection of oriental melon scion grafted onto squash rootstock. Our results are consistent with the findings of Lu and Song (Lu & Song, 1999), who indicated that exogenous plant hormone application could accelerate the rate of plant graft healing.

During the graft union development, the antioxidant defense system, including SOD, PAL, POD, and PPO, was essential for the graft healing process (Gulen et al., 2002; Baxter et al., 2014). PAL and POD enzyme was associated with lignin biosynthesis and tubular molecular formation (Duke et al., 1980; Nakashima et al., 1997; Venema et al., 2008). In addition, PPO not only protected enzymes in plants but also played an important role in lignin biosynthesis. The higher the PPO activity, the longer the existence time of the graft interface between rootstock and scion, which affected the survival of graft healing. (Lavee, 1989; Ali et al., 2006; Zhao et al., 2013). In our study (Figure 2), the NAA treatment significantly enhanced SOD activities of graft junction during the graft union development (Figure 2A). POD and PPO activities were remarkably increased by NAA treatment at the CA and IL stages, respectively. (Figure 2B, 2D). PAL activities were significantly higher than the control at the IL and VB stage under exogenous NAA application (Figure 2C). The results indicated that the exogenous NAA treatment effectively removed the damage caused by reactive oxygen species to the graft interface.

Furthermore, The induction of PPO activities increased some black and brown substances that form an isolated layer produced by the oxidation of phenolics when the plant was cut. The higher the PPO activities, the longer the graft interface's existence time between rootstock and scion, which affected the survival of graft healing (Lopez-Gomez et al., 2007; Li et al., 2019). In our study, NAA treatment had higher PPO activities compared with the control at the IL stage while had lower PPO activities at the CA and VB stage, potentially because the isolated layer disappeared, better formation of callus and the vascular bundle was beneficial to improve the healing speed and survival rate.

IAA, CTK, and GAs are the primary hormones related to callus formation, vascular bundle development, and reconnection (Nieminen et al., 2008; Mauriat & Moritz, 2009; Bishopp et al.,

2011). The appropriate concentration of IAA was added to the undifferentiated tissues, which could promote the formation of vascular tissues (Wetmore & Rier, 1963; Sacha, 1981; Aloni et al., 1990). In our study, the IAA content decreased first and then increased during the graft healing process, consistent with Mo et al. (Mo et al., 2018). When exogenous NAA was applied at the grafting interface, the content of IAA was significantly higher than control at the CA and VB stage (Figure 3A). Our results indicated that the increase of IAA content could promote the development of the xylem and phloem. ZR participates in cell division and vascular differentiation (Hejátko et al., 2009; Bishopp et al., 2011). Our results showed that the ZR content increased first and then decreased with the increase of grafting days in control plants and reached the highest value at the CA stage. Under exogenous NAA treatment, the ZR content was significantly higher than control at the CA stage, which promoted callus formation and accelerated the graft healing process (Figure. 3C). GAs can accumulate in developing xylem tissues of poplar trees (Israelsson et al., 2005; Immanen et al., 2016). This finding coincided with our results of significantly increased GA_3 content during the VB stage (Figure 3B). When NAA was exogenous applied, the content of GA3 was significantly higher than control at the CA and VB stage. The possible reason is that the higher the GA_3 content, the shorter the time for the vascular bundle formation. Our results indicated that after exogenous NAA application, IAA, ZR, and GA_3 were higher than control at the CA and VB stage, suggesting that endogenous regulation was performed under exogenous NAA application. Changes in hormone content affected the graft healing process of oriental melon scion grafted on squash rootstock.

RNA-seq technology has been used to explore the potential transcriptional regulatory mechanisms of the graft healing process (Yong er al., 2002; Cookson et al., 2013; Liu et al., 2015; Chen et al., 2017; Melnyk et al., 2018; Mo et al., 2018; Xu et al., 2021). In order to further analyze the potential molecular networks of exogenous NAA regulating graft healing of oriental melon scion grafted onto squash rootstock, we performed the transcriptome analysis of graft junction at the IL, CA, and VB stage by CK *vs.* NAA using Melon genome and Cucurbita moschata (Rifu) genome, respectively, and deeply excavated the DEGs involved in hormone signal-transduction, ROS scavenging, and vascular bundle formation during graft union development (Figure 7-9). Some reports showed that plant hormone signal-transduction, phenylpropanoid biosynthesis, and phenylalanine metabolism was crucial for graft healing (Qiu et al., 2016; Xu et al., 2017; Mo et al., 2018). Our study similarly found that plant hormone signal-transduction, phenylpropanoid biosynthesis, and phenylalanine metabolism were the overlapping pathways identified at the IL, CA, and VB stage by KEGG pathway enrichment analysis under exogenous NAA treatment.

Previous studies have shown that some genes involved in auxin, cytokinin, and gibberellin signaling are critical regulators for graft union development (Pils & Heyl, 2009; Cookson et al., 2013; Qiu et al., 2016; Mo et al., 2018). Auxin signaling was transmitted via transcriptional regulation of auxin early responsive gene families, including AUX/IAA, Gretchen Hagen 3 (GH3) (Shen et al., 2014; Feng et al., 2015). Several auxin-responsive genes were thought to be regulated during the graft healing formation at the transcriptional level (Zheng et al., 2010; Qiu et al., 2016). Auxin signaling via auxin response factors (ARFs) might be essential for graft union development

(Hardtke & Berleth, 1998). Additionally, cytokinin played an essential role in cell division and vasculature differentiation via the two-component regulatory pathway to active type-B ARR transcription factors (Hardtke & Berleth, 1998; Nieminen et al., 2008; Hejátko et al., 2009; Pils & Heyl, 2009; Aloni et al., 2006; Ikeuchi et al., 2013). In our study, exogenous NAA application significantly promoted the expression of genes involved in auxin signaling, including genes encoding auxin efflux carrier (one melon gene, four cucurbita genes), encoding ARFs (four melon genes, one cucurbita gene), encoding AUX/IAA (four melon genes, four cucurbita genes), and GH3 (four melon genes, two cucurbita genes) during the graft healing process. Meanwhile, genes involved in cytokinin signaling, type-B ARR (one melon gene, three cucurbita genes), CRE1 (one cucurbita gene), AHP (two melon genes, four cucurbita genes), were up-regulated by exogenous NAA. However, we found no significant effects on gibberellin signaling by exogenous NAA application. Moreover, exogenous NAA had different impacts on the melon scion and squash rootstock during graft union development, although exogenous NAA could accelerate graft healing. Besides the hormones, an efficient antioxidant defense system was also crucial in achieving successful grafting (Aloni et al., 2008; Xu et al., 2015; Mo et al., 2018). In the present investigation, exogenous NAA not only promoted the expression of sixteen genes (ten melon genes, six cucurbita genes) encoding POD and two genes (one melon gene, one cucurbita gene) encoding APX but also accelerated the expression of three genes (three melon genes, one cucurbita gene) encoding Prx, two genes (one melon gene, one cucurbita gene) encoding SOD, and three genes (three melon genes) encoding PAL. Exogenous NAA application improved the abilities of ROS scavenging during graft union development.

Correspondingly, the new vascular tissue formation between scion and rootstock marks the success of grafting (Pina & Errea, 2005). This process included a complex physiological and biochemical reaction, such as cell elongation, vascular cell differentiation, and the development of vascular cells that trigger programmed cell death (Ye & Zhong, 2015). Under exogenous NAA application, the vascular bundle connection between melon scion and squash rootstock was earlier than the control. Moreover, through the transcriptome analysis of CK *vs.* NAA at the IL, CA, and VB stage, most genes involved in vascular bundle formation were activated by exogenous NAA (Figure 9). During cell elongation, expansion participated in cell growth and cell wall architecture (De et al., 2015). As expected, six genes expression (two melon genes, four cucurbita genes) were significantly up-regulated by exogenous NAA at the stage. Previous studies indicated that tubulin genes were involved in cell expansion and played an essential role in cell division and elongation (Mendu et al., 1993; Mo et al., 2018). The expression of five cucurbita tubulin genes was enhanced by exogenous NAA at the VB stage. Differentiating vascular cells will conduct with the deposition of cellulose hemicellulose and lignin in the secondary cell wall after the cell elongation. We identified that four cellulose synthase genes (one melon gene, three cucurbita genes) are involved in cellulose synthesis (Suzuki er al., 2006), and one melon cinnamoyl-CoA reductase (CCR) gene is implicated in the phenylpropanoid biosynthesis pathway (Zhao et al., 2013) were up-regulated by exogenous NAA at the VB stage. We also identified sixteen MYB transcription factors (eight melon genes, eight cucurbita genes), participated in the phenylpropanoid biosynthesis pathway as

transcriptional regulators (Stracke et al., 2001), and were significantly improved by exogenous NAA at the VB stage. Hydrolytic enzymes, including aspartic proteinase, cysteine proteinase, and nucleases (exonuclease, ribonuclease), were reported to operate the xylogenesis (Iliev & Savidge, 1999; Courtois-Moreau et al., 2009; Iakimova & Woltering, 2017). In our study, ten genes encoding them were respectively detected with up-regulation under exogenous NAA application at the VB stage. We also detected one cucurbita gene encoding metacaspase involved in plant programmed death and vascular bundle differentiation (Sima et al., 2015; Mo et al., 2018) with higher expression under exogenous NAA application. Obviously, exogenous NAA application strongly triggered the expression of genes involved in vascular bundle formation during the graft healing process of oriental melon grafted onto squash.

Abbreviations

NAA: exogenous naphthylacetic acid
DAG: day after grafting
DEGs: differentially expressed genes
ROS: reactive oxygen species
SOD: superoxide dismutase
POD: peroxidase
PAL: phenylalanine ammonia-lyase
PPO: polyphenol oxidase
IL: isolated layer
CA: callus
VB: vascular bundle
IAA: indole-3-acetic acid
GA: gibberellin
ZR: zeatin riboside
ELISA: Enzyme-Linked Immunosorbent Assay
HPLC: high-performance liquid chromatography
GC-MS: gas-chromatography-mass spectrometry
RNA-seq: transcriptome sequencing
qRT-PCR: quantitative reverse transcription-polymerase chain reaction

Author contributions

CX, FW, and JG participated in the design of the study. CX, FW, JG, SH, XW, and YX conducted the experiments and analyzed the data. CX, FW, and JG drafted the initial manuscript. All authors have given final approval for the publication.

Conflicts of interest

The authors declare that they have no conflict of interest in the present investigation.

Funding

This research was funded by the National Key Research and Development Program of China (2020YFD1000300), the National Natural Science Foundation of China (31401917), the China

Agriculture Research System of Watermelon and Melon (CARS-25), and the Basic Research Project of Liaoning Province (LSNJC202005).

References

Ali, M.B., Khatun, S., Hahn, E.J., Paek, K.Y. 2006. Enhancement of phenylpropanoid enzymes and lignin in phalaenopsis, orchid and their influence on plant acclimatisation at different levels of photosynthetic photon flux. *Plant Growth Regul.* 49 (2-3),137-146. doi:10.1007/s10725-006-9003-z.

Aloni R., Baum S.F., Peterson C.A. 1990. The role of cytokinin in sieve tube regeneration and callose production in wounded Coleus internodes. *Plant Physiology.* 93(3):982-989. doi:10.1104/pp.93.3.982.

Aloni, B., Karni, L., Deventurero, G., Levin, Z., Cohen, R., Katzir, N., Lotan-Pompan, M., Edelstein, M., Aktas, H., Turhan, E. 2008. Physiological and biochemical changes at the rootstock-scion interface in graft combinations between Cucurbita rootstocks and a melon scion. *J. Hortic. Sci. Biotech*. 83, 777-783. https://doi.org/10.1080/14620316.2008.11512460.

Aloni, R., Aloni, E., Langhans, M., Ullrich, C. 2006. Role of cytokinin and auxin in shaping root architecture: Regulating vascular differentiation, lateral root initiation, root apical dominance and root gravitropism. *Ann. Bot*. 97, 883-893. doi:10.1093/aob/mcl027.

Baxter, A., Mittler, R., Suzuki, N. 2014. ROS as key players in plant stress signalling. *J. Exp. Bot.* 65, 1229-1240.

Bishopp A.; Help H.; El-Showk S.; Weijers D.; Scheres B.; Friml J.; Benková E.; Mähönen A.P.; Helariutta Y. 2011. A Mutually Inhibitory Interaction between Auxin and Cytokinin Specifies Vascular Pattern in Roots. *Current Biology*. 21(11):917-26. doi:10.1016/j.cub.2011.04.017.

Chen Z., Zhao J, Hu F., Qin Y., Wang X., Hu G. 2017. Transcriptome changes between compatible and incompatible graft combination of Litchi chinensis by digital gene expression profile. *Scientific Reports*. 7:3954-3954. doi: 10.1038/s41598-017-04328-x.

Cookson S.J., Clemente Moreno M.J., Hevin C., Nyamba Mendome L.Z., Delrot, S., Trossat-Magnin, C., Ollat N. 2013. Graft union formation in grapevine induces transcriptional changes related to cell wall modification, wounding, hormone signalling, and secondary metabolism. *Journal of experimental botany*. 64(10): 2997-3008. doi:10.1093/jxb/ert144.

Courtois-Moreau, C.L., Pesquet, E., Sjödin, A., Muñiz, L., Bollhöner, B., Kaneda, M., Samuels, L., Jansson, S., Tuominen, H. 2009. A unique program for cell death in xylem fibers of Populus stem. *Plant J.* 58, 260-274. doi:10.1111/j.1365-313X.2008.03777.x.

Davis A.R., Perkins-Veazie P., Sakata Y., López-Galarza S., Maroto J.V., Lee S.G., Huh Y.C., Sun Z., Miguel A., King X.X., Cohen R., Lee J.M. 2008. Cucurbit grafting. *Critical Reviews in Plant Sciences*. 27(1):50-74.

De, R.B., Mähönen, A.P., Helariutta, Y., Weijers, D. 2015. Plant vascular development: From early specification to differentiation. *Nat. Rev. Mol. Cell Biol.* 17, 30-40.

518 doi:10.1038/nrm.2015.6.
519 Duke, S.O., Hoagland, R.E., Elmore, C.D. 1980. Effects of glyphosate on metabolism of
520 phenolic compounds. V. L-α-aminooxy-β-phenylalanine ammonia-lyase in soybean
521 seedlings. Plant Physiol. 65 (1), 17-21. doi:10.1104/pp.65.1.17.
522 Enrico Scarpella, Danielle Marcos, Jiří Friml, Thomas Berleth. 2006. Control of leaf vascular
523 patterning by polar auxin transport. *Genes and development*. 20(8):1015-1027.
524 https://doi.org/10.1016/j.ydbio.2006.04.236.
525 Feng S., Yue R., Tao S., Yang Y., Zhang L., Xu M., Wang H., Shen C. 2015. Genome-wide
526 identification, expression analysis of auxin-responsive GH3 family genes in maize (*Zea*
527 *mays* L.) under abiotic stresses. Journal of Integrative Plant Biology. 57:783-795.
528 Fernández-garcía, N., Carvajal, M., Olmos, E. 2004. Graft union formation in tomato plants:
529 peroxidase and catalase involvement. *Ann. Bot.* 93, 53-60. doi:10.1093/aob/mch014.
530 Flaishman M., Loginovsky K., Golobowich S., Lev-Yadun S. 2008. Arabidopsis thaliana as
531 a Model System for Graft Union Development in Homografts and Heterografts. *Journal*
532 *of Plant Growth Regulation*. 27(3):231-9. doi:10.1007/s00344-008-9050-y.
533 Gulen, H., Arora, R., Kuden, A., Krebs, S.L., Postman, J. 2002. Peroxidase isozyme profiles
534 in compatible and incompatible pear-quince graft combinations. *J. Am.Soc. Hortic.*
535 *Sci.*127, 152-157. doi:10.1023/A:1015132615650.
536 Hardtke, C.S., Berleth, T. 1998. The Arabidopsis gene MONOPTEROS encodes a
537 transcription factor mediating embryo axis formation and vascular development. EMBO
538 J. 17, 1405-1411. doi:10.1016/s1369-5266(98)80064-2.
539 Hejátko J., Ryu H., Kim G.T., Dobešová R., Choi S., Choi S.M., Souček P., Horák J.,
540 Pekárová B., Palme K. 2009. The histidine kinases CYTOKININ-INDEPENDENT1
541 and ARABIDOPSIS HISTIDINE KINASE2 and 3 regulate vascular tissue development
542 in Arabidopsis shoots. *Plant Cell.* 21(7):2008-2021.
543 https://doi.org/10.1105/tpc.109.066696.
544 Iakimova, E.T., Woltering, E.J. 2017. Xylogenesis in zinnia (Zinnia elegans) cell cultures:
545 Unravelling the regulatory steps in a complex developmental programmed cell death
546 event. *Planta.* 245, 681-705. doi:10.1007/s00425-017-2656-1.
547 Ikeuchi, M., Sugimoto, K., Iwase, A. 2013. Plant callus: Mechanisms of induction and
548 repression. *Plant Cell*. 25, 3159-3173. https://doi.org/10.1105/tpc.113.116053.
549 Iliev, I., Savidge, R. 1999. Proteolytic activity in relation to seasonal cambial growth and
550 xylogenesis in Pinus banksiana. *Phytochemistry*. 50, 953-960. doi:10.1016/S0031-
551 9422(98)00695-5.
552 Immanen J., Nieminen K., Smolander O.P., Kojima M., Serra J.A., Koskinen P., Bhalerao
553 R.P. 2016. Cytokinin and auxin display distinct but interconnected distribution and
554 signaling profiles to stimulate cambial activity. *Current Biology.* 26(15):1990-1997.
555 doi:0.1016/j.cub.2016.05.053.
556 Ireneusz lesak, Halina lesak, Marta Libik, Zbigniew Miszalski. 2008. Antioxidant
557 response system in the short-term post-wounding effect in Mesembryanthemum

crystallinum leaves. *Journal of Plant Physiology.* 165:2, 127-137. doi:10.1016/j.jplph.2007.03.015.

Irisarri P., Binczycki P., Errea P., Martens H.J., Pina A. 2015. Oxidative stress associated with rootstock-scion interactions in pear/quince combinations during early stages of graft development. *J Plant Physiol.* 176:25-35. doi:10.1016/j.jplph.2014.10.015.

Israelsson M., Sundberg B., Moritz T. 2005. Tissue-specific localization of gibberellins and expression of gibberellin-biosynthetic and signaling genes in wood-forming tissues in aspen. *The Plant Journal.* 44(3):494-504. doi:10.1111/j.1365-313X.2005.02547.x.

J.M. Lee, C. Kubota, S.J. Tsao, Z. Bie, P.H. Echevarria, L. Morra; M. Oda. 2010. Current status of vegetable grafting: Diffusion, grafting techniques, automation. *Scientia Horticulturae* 127:93-105. doi: 10.1016/j.scienta.2010.08.003.

Koepke, T., Dhingra, A. 2013. Rootstock scion somatogenetic interactions in perennial composite plants. Plant Cell Rep. 32 (9): 1321-1337. doi:10.1007/s00299-013-1471-9.

Lavee, S. 1989. Involvement of plant growth regulators and endogenous growth substances in the control of alternate bearing. *Acta Hortic.* 239 (239), 311-322. doi:10.17660/ActaHortic.1989.239.50.

Li Mia, Shuzhen Li, Longqiang Bai, Ali Anwar, Yansu Li, Chaoxing He, Xianchang Yu. 2019. Effect of grafting methods on physiological change of graft union formation in cucumber grafted onto bottle gourd rootstock. *Scientia Horticulturae.* 244, 249-256. doi:10.1016/j.scienta.2018.09.061.

Liu N., Yang J., Fu X., Zhang L., Tang K., Guy K.M., Hu Z., Guo S., Xu Y., Zhang M. 2015. Genome-wide identification and comparative analysis of grafting-responsive mRNA in watermelon grafted onto bottle gourd and squash rootstocks by high-throughput sequencing. *Mol Genet Genomics.* 291:621-33. doi:10.1007/s00438-015-1132-5.

Liu Q., Zhao X., Brecht J.K., Sims C.A., Sanchez T., Dufault N.S. 2017. Fruit quality of seedless watermelon grafted onto squash rootstocks under different production systems. *Journal of the Science of Food and Agriculture*. 97(14):4704-4711. https://doi.org/10.1002/jsfa.8338.

Lopez-Gomez, E., San Juan, M.A., Diaz-Vivancos, P., Beneyto, J.M., Garcia-Legaz, M.F., Hernandez, J.A. 2007. Effect of rootstocks grafting and boron on the antioxidant systems and salinity tolerance of loquat plants (Eriobotrya japonica Lindl.). *Environ. Expt. Bot*. 60(2), 151-158. doi:10.1016/j.envexpbot.2006.10.007.

Lu S.; Song Y. 1999. Relation between phytohormone level and vascular bridge differentiation in graft union of explanted internode autografting. *Chinese Science Bulletin*. 44(20):1874-1878. DOI:10.1007/BF02886344.

Mao X., Cai T., Olyarchuk J.G., Wei L. 2005. Automated genome annotation and pathway identification using the KEGG Orthology (KO) as a controlled vocabulary. *Bioinformatics*. 21:3787-3793. doi:10.1093/bioinformatics/bti430.

Mauriat, M.; Moritz, T. 2009. Analyses of GA20ox- and GID1-over-expressing aspen suggest that gibberellins play two distinct roles in wood formation. *Plant J.* 58(6), 989-1003.

https://doi.org/10.1111/j.1365-313X.2009.03836.x.

Melnyk C.W., Gabel A., Hardcastle T., Robinson S., Miyashima S., Grosse I., Meyerowitz E.M. 2018. Transcriptome dynamics at Arabidopsis graft junctions reveal an intertissue recognition mechanism that activates vascular regeneration. *Proceedings of the National Academy of Sciences*. 115(10): E2447-E2456. https://doi.org/10.1073/pnas.1718263115.

Melnyk CW, Schuster C, Leyser O, and Meyerowitz EM. 2015. A Developmental Framework for Graft Formation and Vascular Reconnection in Arabidopsis thaliana. *Current biology* : CB 25:1306-1318. doi: 10.1016/j.cub.2015.03.032.

Mendu, N., Silflow, C.D. 1993. Elevated levels of tubulin transcripts accompany the GA3-induced elongation of oat internode segments. *Plant Cell Physiol.* 34, 973-983. doi:10.1093/oxfordjournals.pcp.a078533.

Mishra, S., Srivastava, S., Tripathi, R.D., Govindarajan, R., Kuriakose, S.V., Prasad, M.N. 2006. Phytochelatin synthesis and response of antioxidants during cadmium stress in bacopa monnieril. *Plant Physiol. Biochem*. 44 (1), 25-37. doi:10.1016/j.plaphy.2006.01.007.

Mo, Z., Feng, G., Su, W., Liu, Z., Peng, F. 2018. Transcriptomic analysis provides insights into grafting union development in pecan (*Carya illinoinensis*). *Genes*. 9(2), 71. doi:10.3390/genes9020071.

Nakashima, J., Awano, T., Takabe, K., Fujita, M., Saiki, H. 1997. Immunocytochemical localization of phenylalanine ammonia-lyase and cinnamyl alcohol dehydrogenase in differentiating tracheary elements derived from Zinnia mesophyll cells. *Plant Cell Physiol.* 38, 113-123. doi:10.1093/oxfordjournals.pcp.a029140.

Nieminen, K.; Immanen, J.; Laxell, M.; Kauppinen, L.; Tarkowski, P.; Dolezal, K.; Tähtiharju, S.; Elo, A.; Decourteix, M.; Ljung, K. 2008. Cytokinin signaling regulates cambial development in poplar. *Proc. Natl. Acad. Sci.* 105, 20032-20037. https://doi.org/10.1073/pnas.0805617106.

O'Brien T.P., Feder N., McCully M.E. 1964. Polychromatic staining of plant cell walls by toluidine blue O. *Protoplasma*. 59:368-373. doi:10.1007/BF01248568.

Olmos, E., Piqueras, A., Martinez-Solano, J.R., Hellin, E. 1997. The subcellular localization of peroxidase and the implication of oxidative stress in hyperhydrated leaves of regenerated carnation plants. *Plant Sci*. 130, 97-105. doi:10.1016/S0168-9452(97)00214-8.

Olmstead, M.A., Lang, N.S., Lang, G.A., Ewers, F.W., Owens, S.A. 2006. Examining the vascular pathway of sweet cherries grafted onto dwarfing rootstocks. *Hortsci. Publ. Am.Soc.Hortic.Sci.* 41(3), 674-679. doi:10.21273/HORTSCI.41.3.674.

Pils, B., Heyl, A. 2009. Unraveling the evolution of cytokinin signaling. *Plant Physiol*. 151, 782-791. https://doi.org/10.1104/pp.109.139188.

Pina A, and Errea P. 2005. A review of new advances in mechanism of graft compatibility-incompatibility. *Scientia Horticulturae.*106:1-11. doi: 10.1016/j.scienta.2005.04.003.

Polle, A., Otter, T., Seifert, F. 1994. Apoplastic peroxidases and lignification in needles of Norway spruce (Picea abies L.). *Plant Physiol*. 106 (1), 53-60. doi:10.1104/pp.106.1.53.

Qiu, L., Jiang, B., Fang, J., Shen, Y., Fang, Z., Yi, K., Shen, C., Yan, D., Zheng, B. 2016. Analysis of transcriptome in hickory (Carya cathayensis): and uncover the dynamics in the hormonal signaling pathway during graft process. *BMC Genome*. 17 (1), 1-13. doi:10.1186/s12864-016-3182-4.

Ribeiro L.M., Nery L.A., Vieira L.M., Mercadante-Simões M.O. 2015. Histological study of micrografting in passionfruit. *Plant Cell, Tissue and Organ Culture (PCTOC)*. 123:173-181. doi:10.1007/s11240-015-0824-1.

Sacha T. 1981. The control of the patterned differentiation of vascular tissues. Advances in Botanical Research. *Academic Press.* 9:151-262. doi:10.1016/S0065-2296(08)60351-1.

Sánchez-Rodríguez, E., Moreno, D.A., Ferreres, F., Rubio-Wilhelmi, M.M., Ruiz, J.M. 2011. Differential responses of five cherry tomato varieties to water stress: changeson phenolic metabolites and related enzymes. *Phytochemistry*. 72 (8), 723-729. doi:10.1016/j.phytochem.2011.02.011.

Shen C., Yue R., Yang Y., Zhang L., Sun T,. Xu L., Tie S., Wang H. 2014. Genome-wide identification and expression profiling analysis of the Aux/IAA gene family in Medicago truncatula during the early phase of Sinorhizobium meliloti infection. PLoS ONE. 9:e107495-e107495. doi:10.1371/journal.pone.0107495.

Sima, X., Jiang, B., Fang, J., He, Y., Fang, Z., Saravana Kumar, K.M., Ren, W., Qiu, L., Chen, X., Zheng, B. 2015. Identification by deep sequencing and profiling of conserved and novel hickory micrornas involved in the graft process. *Plant Biotechnol. Rep.* 9, 115-124. https://doi.org/10.1007/s11816-015-0349-4.

Stracke, R., Werber, M., Weisshaar, B. 2001. The R2R3-MYB gene family in Arabidopsis thaliana. *Curr. Opin. Plant Biol.* 4, 447-456. https://doi.org/10.1016/S1369-5266(00)00199-0.

Suzuki, S., Li, L., Sun, Y.H., Chiang, V.L. 2006. The cellulose synthase gene superfamily and biochemical functions of xylem-specific cellulose synthase-like genes in Populus trichocarpa. *Plant Physiol.* 142, 1233-1245. doi:10.1104/pp.106.086678.

Turquois, N., Malone, M. 1996. Non-destructive assessment of developing hydraulic connections in the graft union of tomato. *J. Exp. Bot.* 47 (5), 701-707.

Venema J.H., Dijk B.E., Bax J.M., Van Hasselt P.R., Elzenga J.T.M. 2008. Grafting tomato (Solanum lycopersicum) onto the rootstock of a high-altitude accession of Solanum habrochaites improves suboptimal-temperature tolerance. *Environmental and Experimental Botany.* 63(1-3):359-367. https://doi.org/10.1016/j.envexpbot.2007.12.015.

Wang, Y., Kollmann, R. 1996. Vascular Differentiation in the Graft Union of in-vitro Grafts with Different Compatibility-Structural and Functional Aspects. *Journal of plant physiology.* 147(5), 521-533. doi:10.1016/S0176-1617(96)80041-1.

Wetmore R.H., Rier J.P. 1963. Experimental induction of vascular tissues in callus of

678 angiosperms. *American Journal of Botany*. 50(5):418-430.
679 https://doi.org/10.1002/j.1537-2197.1963.tb07210.x.
680 Xu C., Zhang Y., Zhao M., Liu Y., Xu X, Li T. 2021. Transcriptomic analysis of
681 melon/squash graft junction reveals molecular mechanisms potentially underlying the
682 graft union development. *Peer J.* 9:e12569, http://doi.org/10.7717/peerj.12569.
683 Xu, D., Yuan, H., Tong, Y., Zhao, L., Qiu, L., Guo, W., Shen, C., Liu, H., Yan, D., Zheng,
684 B. 2017. Comparative proteomic analysis of the graft unions in hickory (Carya
685 carthayensis) provides insights into response mechanisms to grafting process. *Front.*
686 *Plant Sci.* 8. doi:10.3389/fpls.2017.00676.
687 Xu, Q., Guo, S.R., Li, H., Du, N.S., Shu, S., Sun, J. 2015. Physiological aspects of
688 compatibility and incompatibility in grafted cucumber seedlings. *J. Am. Soc. Hort. Sci.*
689 140, 299-307. doi:10.21273/JASHS.140.4.299.
690 Yang Y-M., Xu C-N., Wang B-M., Jia J-Z. 2001. Effects of plant growth regulators on
691 secondary wall thickening of cotton fibres. *Plant Growth Regulation*. 35:233-237.
692 doi:10.1023/A:1014442015872.
693 Yang, X., Hu, X., Zhang, M., Xu, J., Ren, R., Liu, G. 2016. Effect of low night temperature
694 on graft union formation in watermelon grafted onto bottle gourd rootstock. *Sci.Hortic*.
695 212, 29-34. doi:10.1016/j.scienta.2016.09.010.
696 Ye, Z., Zhong, R. 2015. Molecular control of wood formation in trees. *J. Exp. Bot.* 66, 4119-
697 4131. doi:10.1093/jxb/erv081.
698 Yong Hwa Cheong, Hur-Song Chang, Rajeev Gupta, Xun Wang, Tong Zhu, Sheng Luan.
699 2002. Transcriptional profiling reveals novel interactions between wounding, pathogen,
700 abiotic stress, and hormonal responses in Arabidopsis. *Plant Physiol.* 129:661-677.
701 https://doi.org/10.1104/pp.002857.
702 Young M.D., Wakefield M.J., Smyth G.K., Oshlack A. 2010. Gene ontology analysis for
703 RNA-seq: accounting for selection bias. *Genome biology*. 11:R14-R14. doi:10.1186/gb-
704 2010-11-2-r14.
705 Zhang A., Han D., Wang Y., Mu H., Zhang T., Yan X., Pang Q. 2018. Transcriptomic and
706 proteomic feature of salt stress-regulated network in Jerusalem artichoke (Helianthus
707 tuberosus L.) root based on de novo assembly sequencing analysis. *Planta*. 247, 715-
708 732.
709 Zhao, Q., Nakashima, J., Chen, F., Yin, Y., Fu, C., Yun, J., Shao, H., Wang, X., Wang, Z.-
710 Y., Dixon, R.A. 2013. Laccase is necessary and nonredundant with peroxidase for lignin
711 polymerization during vascular development in Arabidopsis. *Plant Cell*. 25, 3976-3987.
712 https://doi.org/10.1105/tpc.113.117770.
713 Zheng B.S., Chu H.L., Jin S.H., Huang Y.J., Wang Z.J., Chen M., Huang J.Q. 2010. cDNA-
714 AFLP analysis of gene expression in hickory (Carya cathayensis) during graft process.
715 *Tree physiology*. 30(2), 297-303. DOI:10.1093/treephys/tpp102.

Figure 1

Figure 1 Histological changes of graft junction using paraffin sectioning and microscopy method during graft union development.

(A; D), isolation layer stage (IL stage); (B; E), callus tissue stage (CA stage); (C; F), vascular bundles stage (VB stage). SC, scion. RT, rootstock. DAG, days after grafting.

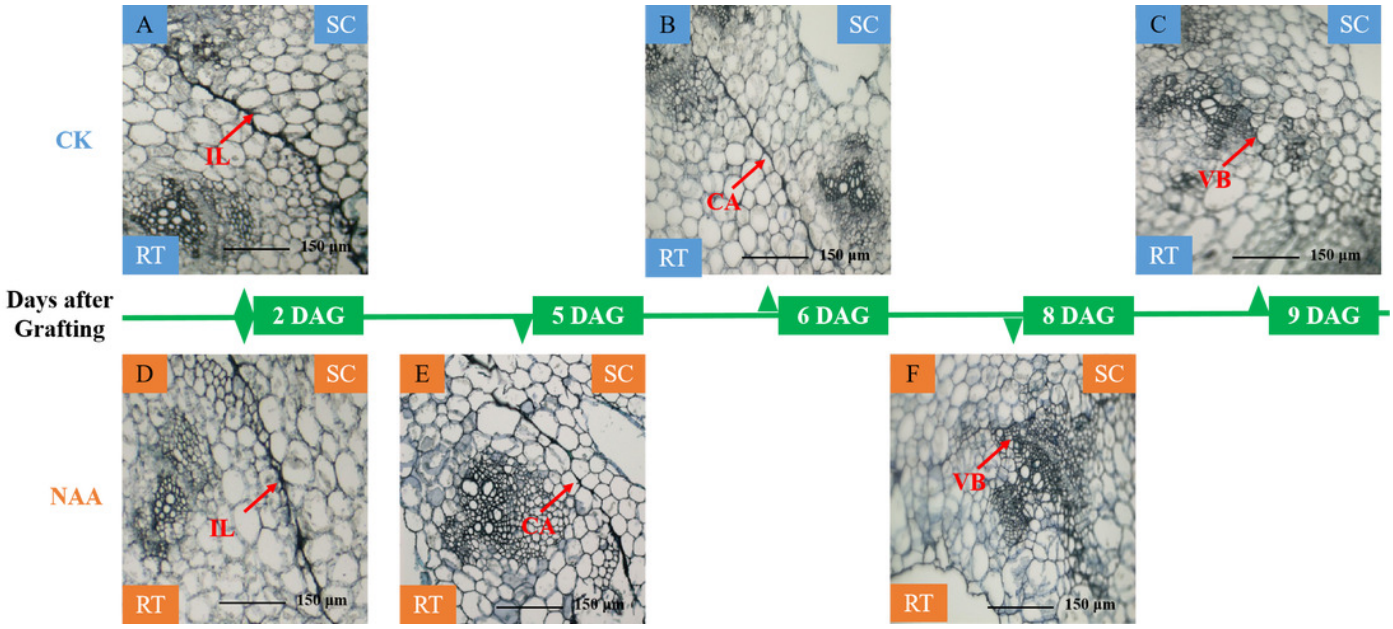

Figure 2

Figure 2 Effects of exogenous NAA application on SOD, POD, PAL, and PPO activities during graft union development.

(A) SOD; (B) POD; (C) PAL; (D) PPO. Different letters indicate significant differences ($p<0.05$). Values are means ± SD, n=3.

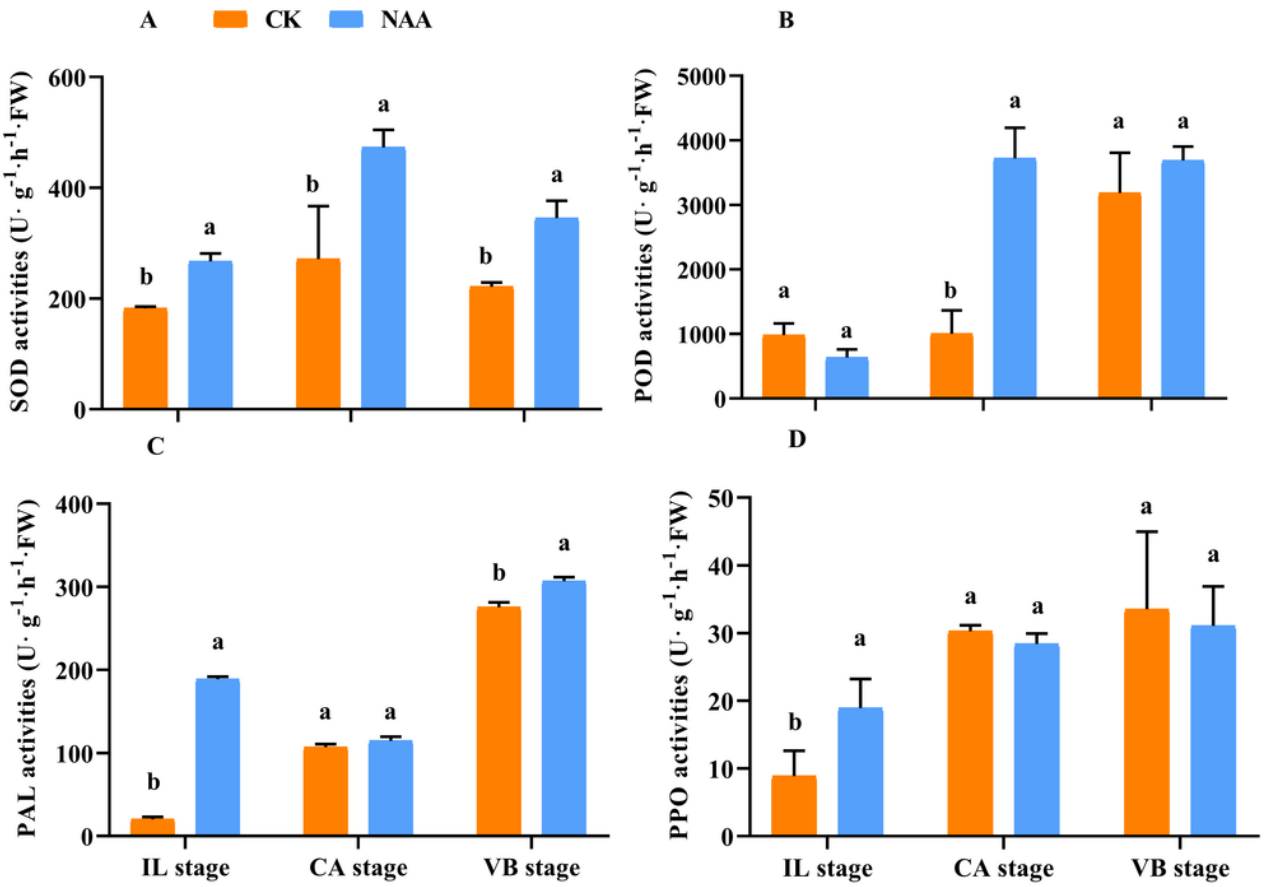

Figure 3

Figure 3 Effects of exogenous NAA application on endogenous hormone contents of IAA, GA, and ZR during graft union development.

(A) IAA; (B) GA_3; (C) ZR. Different letters indicate significant differences ($p<0.05$). Values are means±SD, n=3.

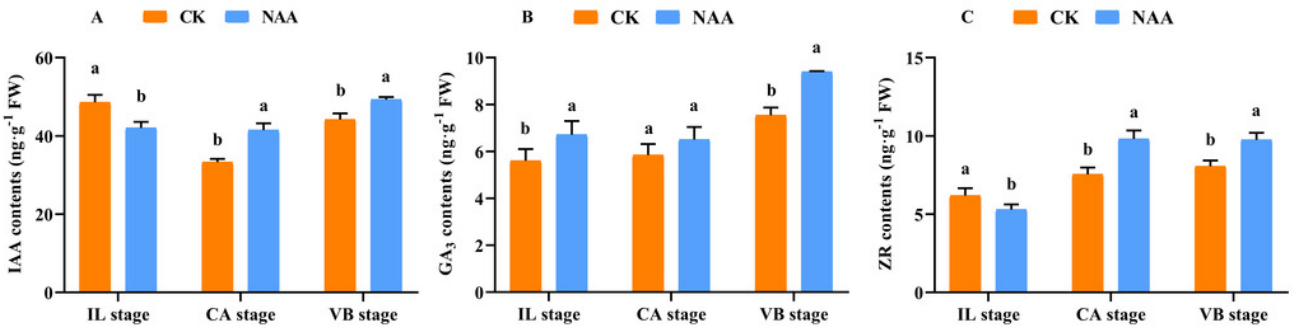

Figure 4

Figure 4 The numbers of DEGs of graft junction at the IL, CA, and VB stage under exogenous NAA application.

(A), CK *vs.* NAA in Melon genome; (B), CK *vs.* NAA in Cucurbita moschata (Rifu) genome.

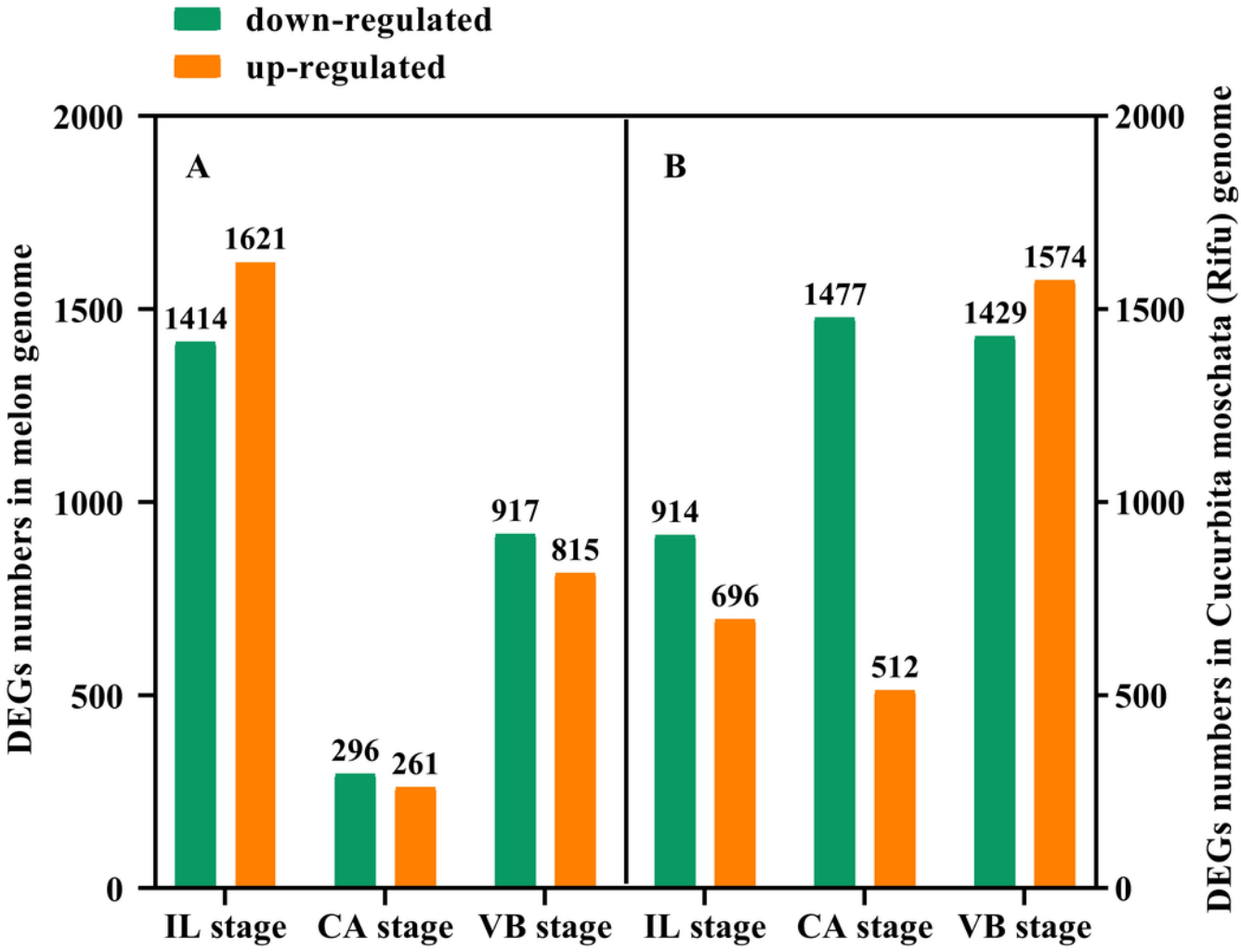

Figure 5

Figure 5 GO functional classification and enrichment analysis of DEGs during graft union development.

(A, C, E) CK *vs.* NAA at the IL, CA, and VB stage using Melon genome. (B, D, F) CK *vs.* NAA at the IL, CA, and VB stage using Cucurbita moschata (Rifu) genome.

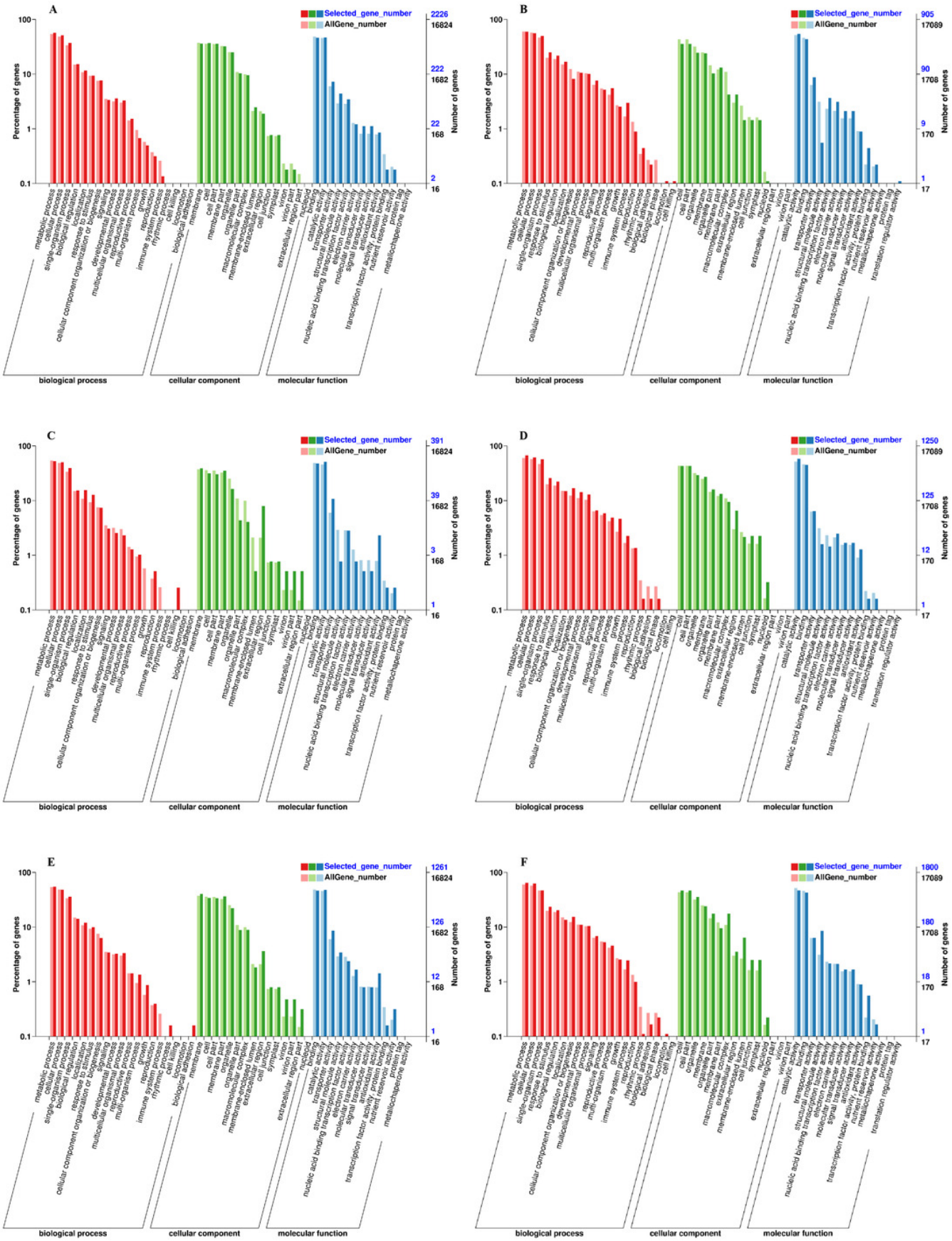
A
Selected_gene_number
AllGene_number
2226
16824
222
1682
22
168
2
16
Percentage of genes
Number of genes
biological process
cellular component
molecular function
B
Selected_gene_number
AllGene_number
905
17089
90
1708
9
170
1
17
Percentage of genes
Number of genes
biological process
cellular component
molecular function
C
Selected_gene_number
AllGene_number
391
16824
39
1682
3
168
1
16
Percentage of genes
Number of genes
biological process
cellular component
molecular function
D
Selected_gene_number
AllGene_number
1250
17089
125
1708
12
170
1
17
Percentage of genes
Number of genes
biological process
cellular component
molecular function
E
Selected_gene_number
AllGene_number
1261
16824
126
1682
12
168
1
16
Percentage of genes
Number of genes
biological process
cellular component
molecular function
F
Selected_gene_number
AllGene_number
1800
17089
180
1708
18
170
1
17
Percentage of genes
Number of genes
biological process
cellular component
molecular function

Figure 6

Figure 6 KEGG pathway enrichment analysis of DEGs during graft union development.

(A, C, E) CK *vs.* NAA at the IL, CA, and VB stage using Melon genome. (B, D, F) CK *vs.* NAA at the IL, CA, and VB stage using Cucurbita moschata (Rifu) genome.

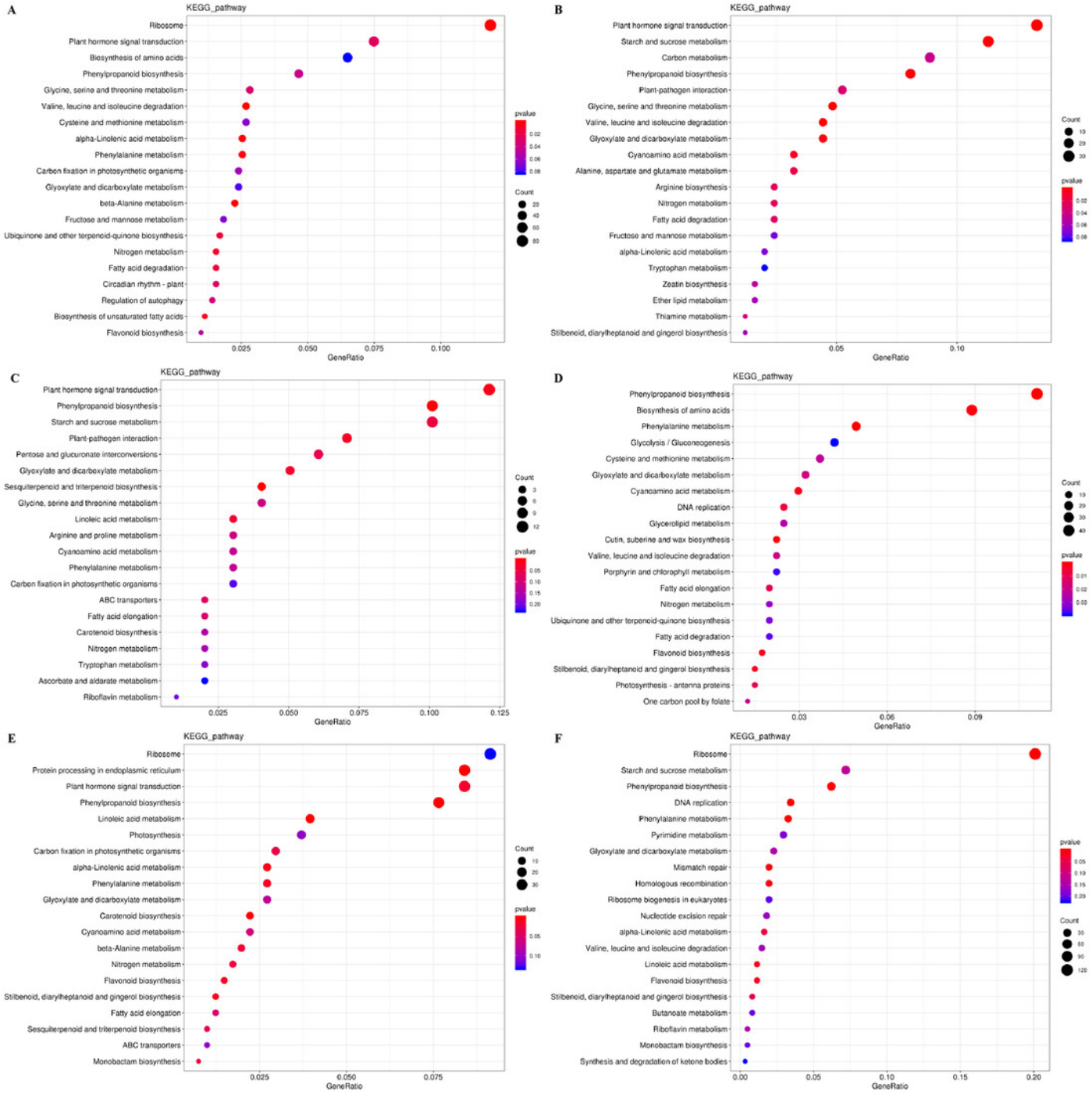
A
KEGG_pathway
Ribosome
Plant hormone signal transduction
Biosynthesis of amino acids
Phenylpropanoid biosynthesis
Glycine, serine and threonine metabolism
Valine, leucine and isoleucine degradation
Cysteine and methionine metabolism
alpha-Linolenic acid metabolism
Phenylalanine metabolism
Carbon fixation in photosynthetic organisms
Glyoxylate and dicarboxylate metabolism
beta-Alanine metabolism
Fructose and mannose metabolism
Ubiquinone and other terpenoid-quinone biosynthesis
Nitrogen metabolism
Fatty acid degradation
Circadian rhythm - plant
Regulation of autophagy
Biosynthesis of unsaturated fatty acids
Flavonoid biosynthesis
0.025 0.050 0.075 0.100
GeneRatio
pvalue
Count
B
KEGG_pathway
Plant hormone signal transduction
Starch and sucrose metabolism
Carbon metabolism
Phenylpropanoid biosynthesis
Plant-pathogen interaction
Glycine, serine and threonine metabolism
Valine, leucine and isoleucine degradation
Glyoxylate and dicarboxylate metabolism
Cyanoamino acid metabolism
Alanine, aspartate and glutamate metabolism
Arginine biosynthesis
Nitrogen metabolism
Fatty acid degradation
Fructose and mannose metabolism
alpha-Linolenic acid metabolism
Tryptophan metabolism
Zeatin biosynthesis
Ether lipid metabolism
Thiamine metabolism
Stilbenoid, diarylheptanoid and gingerol biosynthesis
0.05 0.10
GeneRatio
Count
pvalue
C
KEGG_pathway
Plant hormone signal transduction
Phenylpropanoid biosynthesis
Starch and sucrose metabolism
Plant-pathogen interaction
Pentose and glucuronate interconversions
Glyoxylate and dicarboxylate metabolism
Sesquiterpenoid and triterpenoid biosynthesis
Glycine, serine and threonine metabolism
Linoleic acid metabolism
Arginine and proline metabolism
Cyanoamino acid metabolism
Phenylalanine metabolism
Carbon fixation in photosynthetic organisms
ABC transporters
Fatty acid elongation
Carotenoid biosynthesis
Nitrogen metabolism
Tryptophan metabolism
Ascorbate and aldarate metabolism
Riboflavin metabolism
0.025 0.050 0.075 0.100 0.125
GeneRatio
Count
pvalue
D
KEGG_pathway
Phenylpropanoid biosynthesis
Biosynthesis of amino acids
Phenylalanine metabolism
Glycolysis / Gluconeogenesis
Cysteine and methionine metabolism
Glyoxylate and dicarboxylate metabolism
Cyanoamino acid metabolism
DNA replication
Glycerolipid metabolism
Cutin, suberine and wax biosynthesis
Valine, leucine and isoleucine degradation
Porphyrin and chlorophyll metabolism
Fatty acid elongation
Nitrogen metabolism
Ubiquinone and other terpenoid-quinone biosynthesis
Fatty acid degradation
Flavonoid biosynthesis
Stilbenoid, diarylheptanoid and gingerol biosynthesis
Photosynthesis - antenna proteins
One carbon pool by folate
0.03 0.06 0.09
GeneRatio
Count
pvalue
E
KEGG_pathway
Ribosome
Protein processing in endoplasmic reticulum
Plant hormone signal transduction
Phenylpropanoid biosynthesis
Linoleic acid metabolism
Photosynthesis
Carbon fixation in photosynthetic organisms
alpha-Linolenic acid metabolism
Phenylalanine metabolism
Glyoxylate and dicarboxylate metabolism
Carotenoid biosynthesis
Cyanoamino acid metabolism
beta-Alanine metabolism
Nitrogen metabolism
Flavonoid biosynthesis
Stilbenoid, diarylheptanoid and gingerol biosynthesis
Fatty acid elongation
Sesquiterpenoid and triterpenoid biosynthesis
ABC transporters
Monobactam biosynthesis
0.025 0.050 0.075
GeneRatio
Count
pvalue
F
KEGG_pathway
Ribosome
Starch and sucrose metabolism
Phenylpropanoid biosynthesis
DNA replication
Phenylalanine metabolism
Pyrimidine metabolism
Glyoxylate and dicarboxylate metabolism
Mismatch repair
Homologous recombination
Ribosome biogenesis in eukaryotes
Nucleotide excision repair
alpha-Linolenic acid metabolism
Valine, leucine and isoleucine degradation
Linoleic acid metabolism
Flavonoid biosynthesis
Stilbenoid, diarylheptanoid and gingerol biosynthesis
Butanoate metabolism
Riboflavin metabolism
Monobactam biosynthesis
Synthesis and degradation of ketone bodies
0.00 0.05 0.10 0.15 0.20
GeneRatio
pvalue
Count

Figure 7

Figure 7 Expression patterns of DEGs involved in hormone signal-transduction.

The values of log_2 fold change were shown in the heat map.

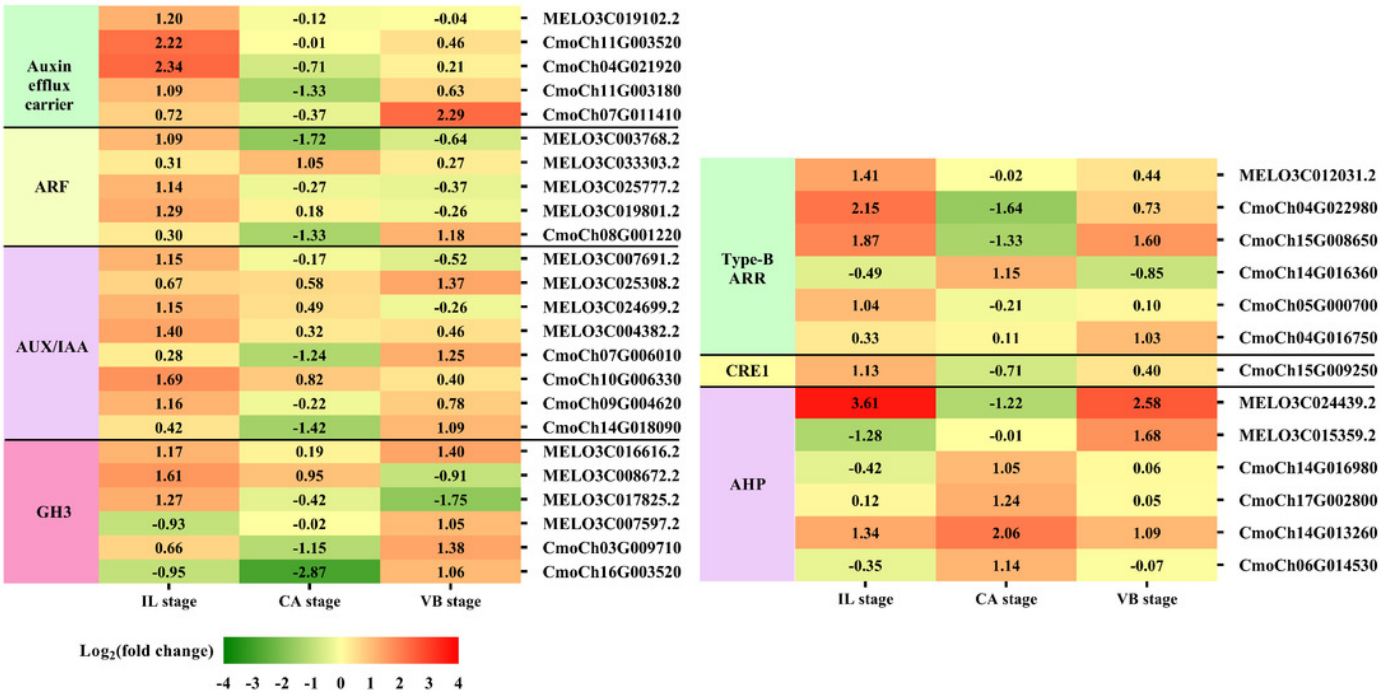

Figure 8

Figure 8 Expression profiles of DEGs involved in ROS scavenging.

The values of log_2 fold change were shown in the heat map.

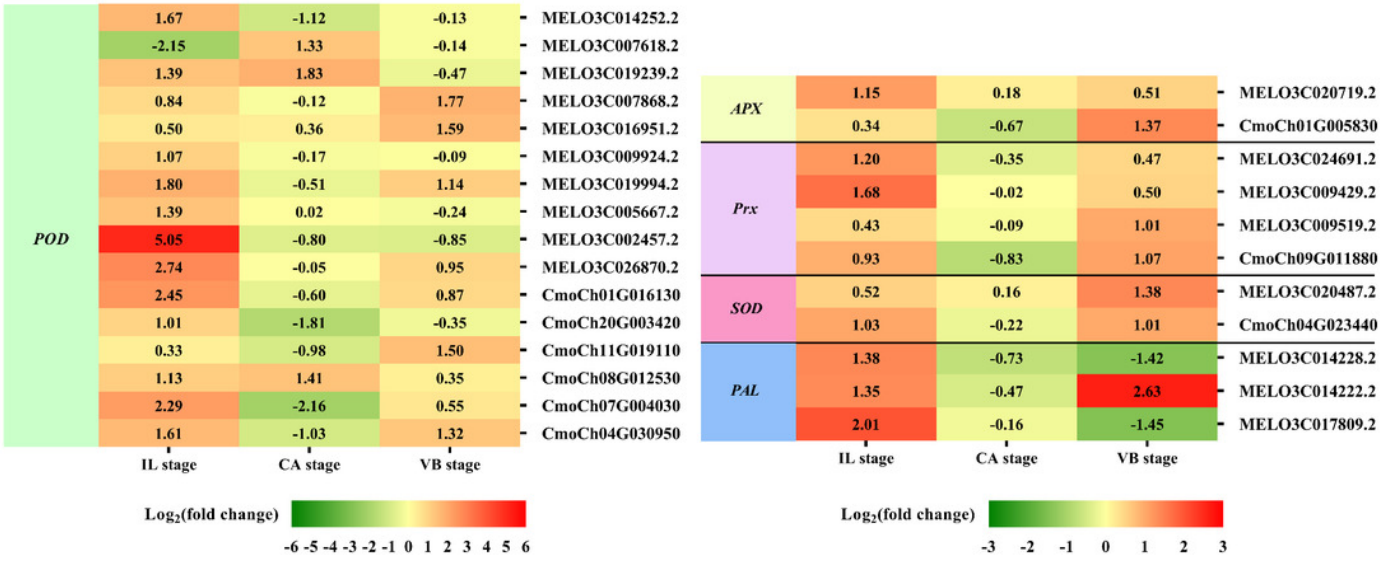

Figure 9

Figure 9 Expression profiles of DEGs involved in vascular bundle formation.

The values of $\log_2$ fold change were shown in the heat map.

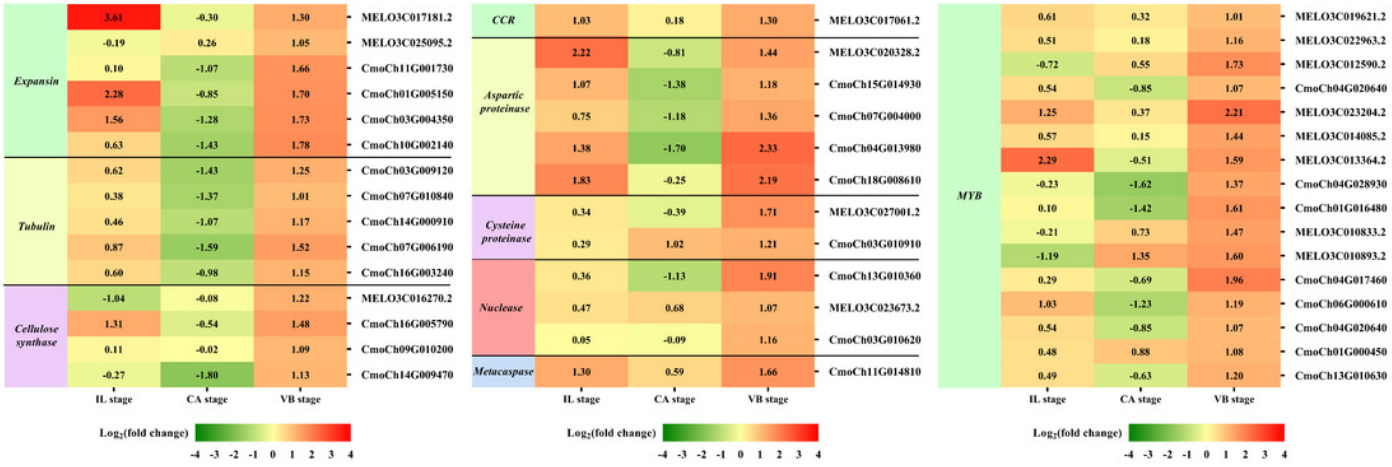

Figure 10

Figure 10 Verification of differentially expressed genes by qRT-PCR.

Different letters indicate significant differences ($p<0.05$). Values are means±SD, n=3.

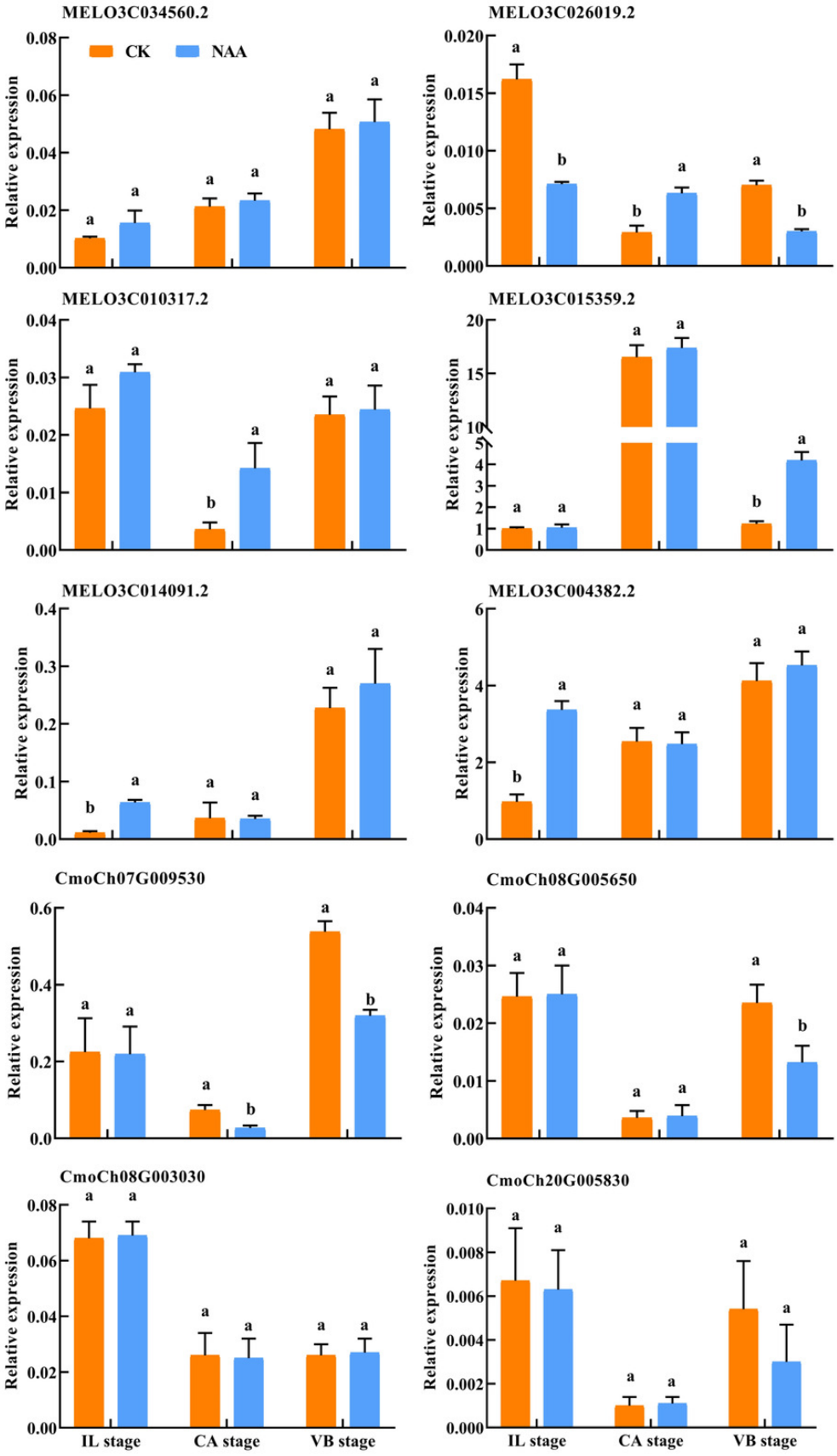
MELO3C034560.2
CK
NAA
Relative expression
MELO3C026019.2
MELO3C010317.2
MELO3C015359.2
MELO3C014091.2
MELO3C004382.2
CmoCh07G009530
CmoCh08G005650
CmoCh08G003030
CmoCh20G005830
IL stage
CA stage
VB stage